PHYSICAL REVIEW A VOLUME 37, NUMBER 12 JUNE 15, 1988

Resonant multiphoton ionization of atomic hydrogen

Y. Gontier
Service de Physique des Atomes et des Surfaces, Centre d'Études Nucléaires de Saclay, 91191 Gif-sur-Yvette Cédex, France

N. K. Rahman
Dipartimento di Scienze Chimiche, Universita di Trieste, Piazzale Europa 1, Trieste, Italy

M. Trahin
Service de Physique des Atomes et des Surfaces, Centre d'Études Nucléaires de Saclay, 91191 Gif-sur-Yvette Cédex, France

(Received 29 October 1987)

The resonantly enhanced multiphoton ionization of atomic hydrogen is studied for the case of four-photon ionization (three-photon resonant). The time-dependent probabilities, the shape of the resonance profile at different intensities, and the nonlinear index are computed for coherent light at frequencies around the resonance (365 nm). The systematic dependence of the cross section as a function of the principal quantum number of the resonant state (as this tends towards the Rydberg states) is investigated at zero detuning. The probabilities of absorption of one photon more than necessary for the four-photon ionization process (resonantly enhanced above-threshold ionization) is computed and the relevant branching ratios are examined. Then it is shown that the effect of the spatio-temporal structures of the laser pulse is to red shift the maximum of the resonance profile, whereas that of an ideal chaotic light is to blue shift and broaden the resonance peak. The shape, shift, and width of the profile resulting from both these effects are in very fair agreement with the experimental ones.

I. INTRODUCTION

Resonantly enhanced multiphoton ionization (REMPI) is an important sub-branch of research in the general area of multiphoton processes which has been the object of numerous experimental and theoretical investigations for the last few years.[1] The principal characteristics of REMPI lie in the fact that around the resonance, the ionization probability is much larger than what may be termed the background probability, which itself is a subject of much theoretical and experimental activity. The importance of REMPI resides also in the fact that the shifts and the widths of the resonance peaks, which are functions of the strength of the external electromagnetic field as well as its coherence properties, reveal dynamics of the absorption process of photons while the system ends up in the continuum. REMPI has been, therefore, the subject of a large number of investigations.[2–11]

The frequencies that have been available experimentally to date to study REMPI for atoms along with the accessibility of the atoms themselves have restricted these studies predominantly to alkali-metal and alkaline-earth-metal atoms. This lopsided imbalance in favor of these atoms also contrasts sharply with the dearth of experiments regarding what we consider the fundamental atom, i.e., the hydrogen atom *vis-à-vis* REMPI. Fortunately, this situation is changing, and one notes that experiments with the hydrogen atoms are being reported or are being performed. Two recent experiments on H concern four-photon ionization, with three-photon absorption being the resonance condition. If one goes back in the theoretical literature, one notes that, while a great deal has been achieved regarding nonresonant multiphoton ionization (MPI) for H, utilizing a variety of theoretical techniques, few calculations exist regarding REMPI.[6,11] Calculations that have been done for the nonresonant cases are inappropriate for REMPI, since the amplitudes of REMPI that are calculated with these techniques simply lead to divergences. The situation being such, we report here a detailed investigation of REMPI for H, limiting ourselves mostly to that frequency range where two experiments have been performed.[12,13] In other words, we treat three-photon-resonant four-photon processes [Fig. 1(a)]. As will be clear from a perusal of this paper, we shall cover an aspect of REMPI that goes much beyond the limits imposed in these experiments. Our investigations for the above processes consist of calculations of the following quantities: (1) time dependence of the ionization probability, (2) shape of the resonance profile, (3) intensity dependence of the ionization probability $P(I)$ around the resonance, (4) nonlinear index $K=d[\ln P(I)]/dI$ in the same energy range, (5) dependence of the probability on the principal quantum number of the resonant level, (6) the branching ratio of the photoelectrons between four-photon and five-photon absorption with the same frequency of light, (7) effect of the spatio-temporal pulse shape, and (8) ionization probability for thermal or chaotic light. From the above list, it is clear that we shall be presenting a large number of results of quite extensive computations. Fortunately, our paper is mostly that. There is no need for an excessively lengthy paper where the formalism, the theory, and the results all have to be

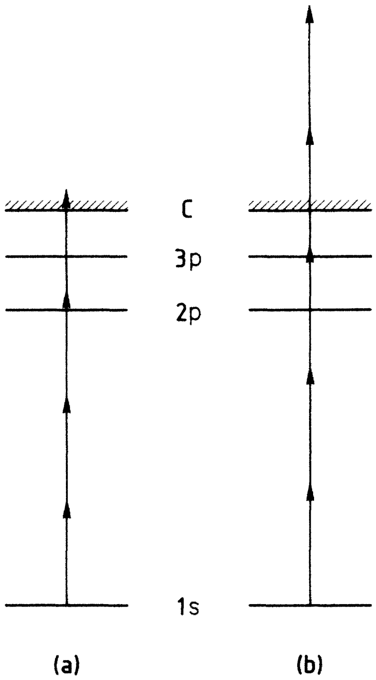

FIG. 1. (a) Four-photon ionization of atomic hydrogen. The $2p$ state is the resonant one, which may be replaced by a general np state for $n \leq 10$. When $2p$ is the resonant state, the process is at the threshold energy of the electron. (b) Four-photon ionization with $3p$ being the resonant state and an additional absorption of one photon (resonant above-threshold ionization).

presented. The basic theory need not be expounded in any detail, since this has already been done elsewhere.[10] Only the results of calculations relevant for the list above will be presented. It will be shown how these calculations may be of help in understanding experiments that have been performed and some interesting future experiments. Since these calculations are in some sense exact, these experiments are indicated for satisfactory understanding of the H atom *vis-à-vis* aspects of multiphoton ionization that lie within the scope of these calculations. Sections II–IV contain the exposition of our results. Section II, after a brief outline of the basic theory, reports the time dependence of the resonant-ionization probability with the initial state being the ground state of H atom and the $2p$ state being the resonant state. One then considers the linear (in time) regime of the probability. This is most often the accessible experimental domain. In this domain, the shape of the resonance profile, the dependence on intensity of this profile, and the well-known nonlinear index around the resonance are all calculated and reported. Section III deals with two problems concerned with some recent aspects of REMPI. Calculations are presented for the cross sections of ionization as a function of the principal quantum number of the resonant state. We uncover some remarkably general features for these. Next, the probability of the absorption of an additional photon in the continuum is treated [Fig. 1(b)]. We report the branching ratio between $(3+1+1)$-photon ionization (three-photon resonant, four-photon ionization, one additional photon absorbed) to the $(3+1)$-photon ionization. The calculation of the branching ratio between these two processes is extended to a set of resonant levels in order to obtain the systematic (if any) variation of this branching ratio to the principal quantum number of the resonant state. Section IV is concerned with the effect of the realistic spatio-temporal pulse shape of lasers currently in use on the results presented in Secs. II and III. This is of great experimental interest. Also in Sec. IV, results are presented for thermal or chaotic light *vis-à-vis* REMPI, one of those cases of much interest as far as optical physics is concerned. A brief section (Sec. V) with some pertinent remarks concludes the paper.

II. BASIC IONIZATION PROBABILITY

In this section, the basic results of a four-photon ionization calculation of the H atom with the $2p$ state as the resonant state is reported. By the term basic, we mean that the ionization is due to an idealized square monomode pulse. The photon frequency is approximately 274 19.7 cm^{-1} for the ionization to occur with the $2p$ being the state that would allow a three-photon bound-bound transition. The basic expressions for the ionization probability need not be derived here, since they have been derived elsewhere.[10] However, before the expressions necessary for computations are written down, a brief guide to these expressions must be given in order to appreciate the results.

Given that the atom can be described by the Hamiltonian H_0 [the Green's function thereof being $G_0 = 1/(E - H_0)$] and the interaction Hamiltonian is $V = V^+ + V^-$, the generic mth-order operator may be defined as

$$M = V^- G_0 V^- G_0 \cdots V^- G_0 V^- \ , \tag{1}$$

where V^- occurs m times. The shift width of the resonating state $|\,j\,\rangle$ is then given by

$$\Delta_j - i\gamma_j/2 = (I/I_0)(\langle j\,|\,D^+ G_0 D^-\,|\,j\,\rangle + \langle j\,|\,D^- G_0 D^+\,|\,j\,\rangle) \ , \tag{2}$$

where $V^{\pm} = \sqrt{(I/I_0)}D^{\pm}$, with I being the laser intensity in W/cm^2, $I_0 = 1.4 \times 10^{17}$ W/cm^2 and $D^{\pm}$ being the dipole operator.

We shall also need the shift of the initial state $|\,i\,\rangle$,

$$\Delta_i = (I/I_0)(\langle i\,|\,D^+ G_0 D^-\,|\,i\,\rangle + \langle i\,|\,D^- G_0 D^+\,|\,i\,\rangle) \ . \tag{3}$$

The width γ_i, which arises from eighth-order matrix elements, may be neglected compared to γ_j, which arises from second-order ones. The nondiagonal matrix element of interest is

$$R_{ij} = (I/I_0)^{3/2} \langle i\,|\,D^- G_0 D^- G_0 D^-\,|\,j\,\rangle \ . \tag{4}$$

Define further a detuning, containing the shifts

$$\delta = (E_i + \Delta_i) - (E_j + \Delta_j) \ . \tag{5a}$$

A global width and a width difference are also defined,

$$\Gamma=(\gamma_i+\gamma_j)/2\ , \tag{5b}$$

$$\rho=(\gamma_i-\gamma_j)/2\ . \tag{5c}$$

With the quantities above, we define the following:

$$\beta_1=|\delta|[1+2R_{ij}^2/(\delta^2+\rho^2)]\ , \tag{6a}$$

$$\beta_2=\epsilon|\rho|[1-2R_{ij}^2/(\delta^2+\rho^2)]\ , \tag{6b}$$

where $\epsilon=\delta/|\delta|$.

The time-dependent ionization probability is then given by

$$P(t,I)=1-F\{(A-2B)e^{-(\Gamma-\beta_2)t}+(A+2B)e^{-(\Gamma+\beta_2)t}-2[C\cos(\beta_1 t)+2D\sin(\beta_1 t)]e^{-\Gamma t}\}\ , \tag{7a}$$

where

$$F=[4(\delta^2+\rho^2)]^{-1}\ , \tag{7b}$$

$$A=2(\delta^2+\rho^2)+4R_{ij}^2\ , \tag{7c}$$

$$B=\rho\beta_2-\delta\beta_1\ , \tag{7d}$$

$$C=4R_{ij}^2\ , \tag{7e}$$

$$D=\rho\beta_1+\delta\beta_2\ . \tag{7f}$$

The expression in Eq. (7a) is our basic expression from which all the relevant quantities are to be obtained. The computations are performed to obtain the expressions given in Eqs. (2), (3), and (4) with the now standard technique of solving an ensemble of coupled hierarchical differential equations.[14]

These are then utilized to obtain $P(t)$. Results of the calculations are shown in Fig. 2. These curves are useful for studying the dependence of the process as a function of the duration of the interaction. Furthermore, it helps us to understand in what region of a hypothetical laser-pulse duration one may expect to have linear dependence of time and, therefore, in which time domain rates of ionization that are independent of time may be defined. As a concrete example, the experiment in Ref. 12 has utilized a 9-nsec pulse which falls in that linear regime.

The expression for the time-dependent probability is essentially linear over a quite large interval. The linear time dependence results under certain algebraic conditions, which for our case are

$$\Gamma+|\beta_2|>\Gamma\gg\Gamma-|\beta_2|\ ,\quad \rho^2\gg C\ .$$

Under these conditions, one can reduce Eq. (7a) to

$$P(t,I)=R_{ij}^2\gamma_j t/(\delta^2+\gamma_j^2/4)\ , \tag{8}$$

and the time-dependent rate is directly obtained by dividing by t. The resonance profile is best studied in that condition as a function of intensity.

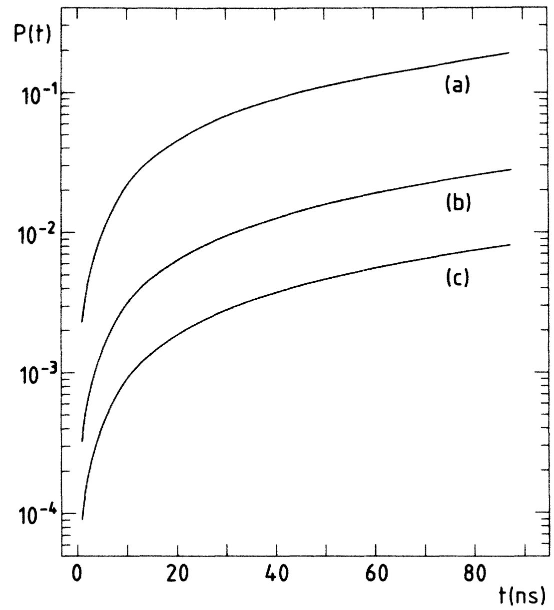

FIG. 2. Four-photon ionization probability of H as a function of time for three near-resonant photon energies (a) 27 421.8 cm^{-1}, (b) 27 423.8 cm^{-1}, and (c) 27 425.8 cm^{-1}. The laser intensity is $I=3\times10^{10}\ \text{W/cm}^2$.

In Fig. 3, the profile of the resonance is plotted for a square pulse having three different intensities ($I=1\times10^{10}$, 2×10^{10}, $3\times10^{10}\ \text{W/cm}^2$). The probabilities increase with the increase of intensity (the denominator cannot keep pace with the numerator, where $R_{ij}^2\gamma_j$ increases faster than γ_j^2), while the widths of the profile become larger with the increase of γ_j. It is worthwhile to compare these profiles with those for the cesium atom which have been calculated before.[10] The shapes of the H resonance profile are much broader while those of Cs are sharper. Apart from attributing the difference between

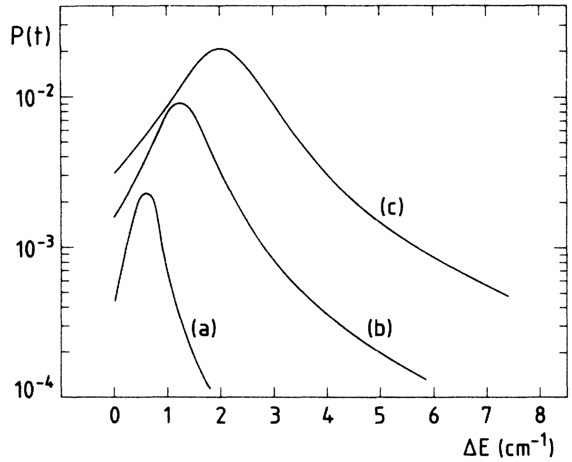

FIG. 3. Four-photon ionization probability of H as a function of the photon energy. Notice that the process has an energetic threshold for photons at $E_p=27\,419.7\ \text{cm}^{-1}$ ($\Delta E=0$). The interaction time τ is 9 nsec and the curves are drawn at intensities (a) $I=10^{10}\ \text{W/cm}^2$, (b) $I=2\times10^{10}\ \text{W/cm}^2$, and (c) $I=3\times10^{10}\ \text{W/cm}^2$.

these two systems to the computed values of the quantities that go into Eq. (7a), an alternate manner of viewing this is that of curve crossing of the dressed atomic levels. The crossing of H occurs at a much larger angle than that for Cs. A particular aspect of these resonance curves should be kept in mind. The H atom is an exceptional atom in a particular sense for MPI. The frequency ($27\,419.7$ cm^{-1}) is the frequency for which the state $2p$ would be the resonant state with the absorption of three photons for a four-photon ionization process. It is also the threshold frequency for this ionization, i.e., below this frequency, the ionization process is a five-photon process, the four-photon ionization being energetically forbidden. At the resonant frequency ω_R, one may expand the probability around this frequency,

$$P(\omega,I)=P(\omega_R,I)+(\omega-\omega_R)P'(\omega_R,I)\ .$$

If $P'(\omega_R,I)$ does not vanish, one expects a linear region in frequency. From the results of our calculations, we see that for the three intensities at which computations have been done, $P'(\omega_R,I)$ are all positive and the probabilities do increase linearly. The slopes are all different and the values of these slopes are functions of the intensities.

Another aspect of the same resonance is obtained if one calculates the probabilities as a function of intensity for fixed frequency (Fig. 4). At $27\,419.7$ cm^{-1}, the intensity dependence between 3×10^9 and 5×10^{11} W/cm^2 is linear for all practical purposes. Such calculations have been done between $27\,418.8$ and $27\,429.8$ cm^{-1} at six different frequencies. The dependence on the intensities for five frequencies that were calculated all show a certain structure. Beyond $27\,429.8$ cm^{-1}, there is again a linear dependence on intensity. Perusal of Fig. 3 firstly shows that the peak of the probability for $I=3\times10^{10}$ is at $27\,421.7$ cm^{-1}. Therefore we expect some nontrivial variation to occur on both sides of this frequency. This is what is seen in Fig. 4. How these curves should vary between these values is of experimental interest and our calculations provide predictions for such. The nonmonotonic variation that one observes around the resonant frequency is to be compared also to that calculated for Cs. While for the shape of the resonance profile, it is not difficult to intuitively expect such variation, the shape of the intensity-dependent curves is not amenable to simple interpretations.

The last quantity that we report in this section is the nonlinear index K, which is a characteristic index for multiphoton resonant processes (Fig. 5). These are to be computed around the resonance value which, as was indicated earlier, is also the threshold frequency for this ionization. The profile of resonance shows (Fig. 3) that the maximum shifts by about 2 cm^{-1} ($I=3\times10^{10}$ W/cm^2) from the threshold value. K has been calculated for constant probabilities of 10^{-3} and 10^{-4} at the vicinity of this threshold. The index K is 4 for nonresonant four-photon processes in general. For the calculation shown, this value is never reached, indicating how broad the resonance profile is for these two probabilities. The maximum value of K is 5.6 (for a detuning $\Delta E=0.6$ cm^{-1}

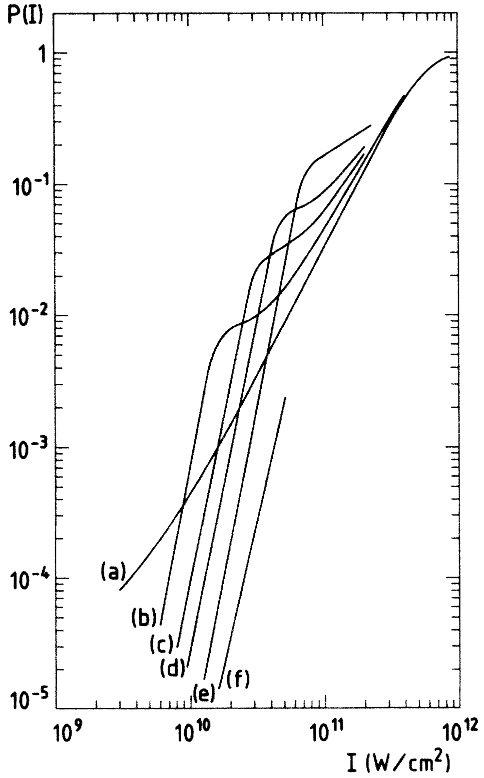

FIG. 4. Probability of the same process as that in Figs. 2 and 3, given as a function of intensity for six different photon energies: (a) $27\,419.8$ cm^{-1}, (b) $27\,420.8$ cm^{-1}, (c) $27\,421.8$ cm^{-1}, (d) $27\,422.8$ cm^{-1}, (e) $27\,424.8$ cm^{-1}, and (f) $27\,429.8$ cm^{-1}. The interaction time is 9 nsec.

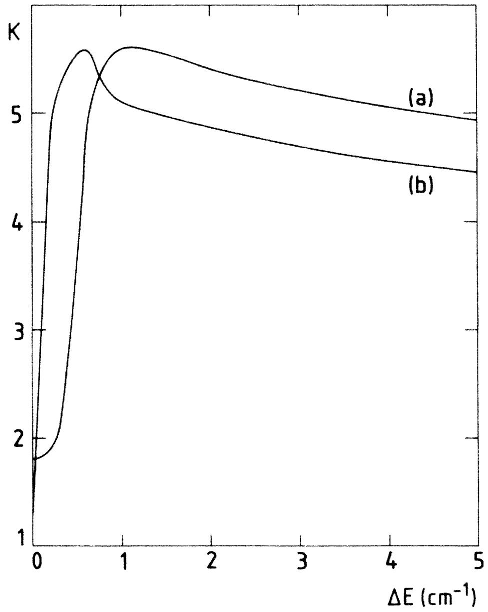

FIG. 5. Order of nonlinearity K of the same processes as those in Figs. 1–4, shown as a function of the resonance-detuning ΔE cm^{-1} for two different constant probabilities: (a) $P=10^{-3}$ and (b) $P=10^{-4}$ ($\tau=9$ nsec).

and a probability $P=10^{-4}$), and remains the same for the probability 10^{-3} (but now at $\Delta E = 1$ cm^{-1}), indicating also that the resonance profile shifts towards the blue. On the red end of the maxima, the variation of K is indeed very steep. The sharp decline dipping down to less than 2 is indeed only revealed by the computation and does not appear to be easily predictable analytically. The K index at the threshold for hydrogen may also be discussed in relation to other typical atomic cases. One expects, barring the hydrogen atom, the threshold to be at nonresonant frequencies. Thus, the index would be $K=N$, where N is the order of the multiphoton process. One also shows that at the threshold, the probability is constant for hydrogen.[15,16] The four-photon ionization is an atypical case where, while the probability of ionization goes to a constant at the threshold, the index K will jump from $K<2$ to $K>5$ (with $\Delta K>3$), while the probability of ionization will show a discontinuity, as expected for a transition from a four-photon to a five-photon process. The usual nonresonant ionization process will show the discontinuity with $\Delta K=1$ across the threshold.

III. SYSTEMATIC DEPENDENCE ON RESONANT STATES

The results of all the calculations reported above are expected to be useful for quantitative comparison with other calculations as well as for comparison with experimental data, if and when they become available. All of these rather involved computations refer to the $2P$ state as the resonant state. An interesting question is how the REMPI processes depend on the quantum numbers of the resonant states. This question is especially relevant for the hydrogen atom, since exact calculations can be performed. The results of a systematic study of this problem are presented here. The qualitative trend, if any, could also be of help in understanding the systematics of some other atoms such as the alkali-metal atoms, for which experiments may be easier to perform. We report here the results of our calculations performed for all the resonant states from $n=3$ to 10 (n is the principal quantum number). Our results will show that even for these not very large values of n, a systematic trend emerges which converges towards the behavior expected for the Rydberg states. We would further add that real experiments with Rydberg states cannot be expected to fully reflect the results of our calculations since, apart from the intrinsic limitations of the lowest-order perturbation theory, additional effects such as those due to blackbody radiation may lead to complications. This is why the calculations have been limited to not too large values of n. The calculations are divided into two parts: (a) four-photon ionization from the ground state [Fig. 1(a)], and (b) five-photon ionization with the last photon being absorbed in the continuum [Fig. 1(b)]. This second calculation is therefore a calculation of the above-threshold ionization as well.

(a) Resonant four-photon ionization as a function of n (REMPI). The results of the calculation are shown in Fig. 6 and Table I. Referring to Eq. (8) with $\delta=0$, we see that the transition probability per unit time can be written as

$$W^{(4)}=4\,|R_{ij}|^2/\gamma_j^{(1)}\ , \tag{9}$$

where

$$|R_{ij}|^2=(I/I_0)^3\,|\langle 1s\,|D^-G_0D^-G_0D^-|\,np\rangle|^2\ , \tag{10a}$$

and

$$\gamma_j^{(1)}=2\pi(I/I_0)(\,|\langle E,s\,|D^-|\,np\rangle|^2 + |\langle E,d\,|D^-|\,np\rangle|^2)\ . \tag{10b}$$

The dependence on n arises both in R_{ij} and $\gamma_j^{(1)}$. Now R_{ij} is essentially the three-photon excitation probability to the state $j\equiv|\,np\rangle$. With the increase in n, this decreases, somewhat in analogy with one-photon excitation as a function of n (this latter varies inversely as the cube of n). $\gamma_j^{(1)}$ is akin to the photoionization probability from the state $|\,np\rangle$ which decreases with n. The ratio of these two functions is an increasing function of n. The increase, however, is rather small as n reaches the value 10, and the probability of ionization reaches a plateau around that value for n.

(b) Resonant five-photon ionization (REATI). At intensities at which four-photon ionization signals are measured, it is also of interest to measure the five-photon absorption probability. This means that one more photon is absorbed, this photon being absorbed entirely in the continuum. Such processes in which one or more photons are absorbed in the continuum in conjunction with usual

TABLE I. Numerical values of the quantities defined in Sec. III for the principal quantum numbers $n=2$ to 10. R is the branching ratio between five- and four-photon processes.

n	$10^{48}\,|R_{ij}|^2/I^3$	$10^{17}\gamma_j^{(1)}/I$	$10^{32}\gamma_j^{(2)}/I^2$	$10^{31}W^{(4)}/I^2$	$10^{46}W^{(5)}/I^3$	$10^{15}R$
2	11.97	75.38	146.9	0.63	1.24	1.96
3	4.192	9.420	27.11	1.78	5.15	2.89
4	2.626	3.126	7.786	3.36	8.37	2.49
5	1.544	1.443	3.356	4.28	9.96	2.33
6	0.962	0.790	1.776	4.87	10.9	2.25
7	0.634	0.482	1.057	5.26	11.5	2.19
8	0.438	0.316	0.685	5.54	12.0	2.17
9	0.314	0.219	0.471	5.74	12.3	2.15
10	0.232	0.158	0.338	5.89	12.6	2.14

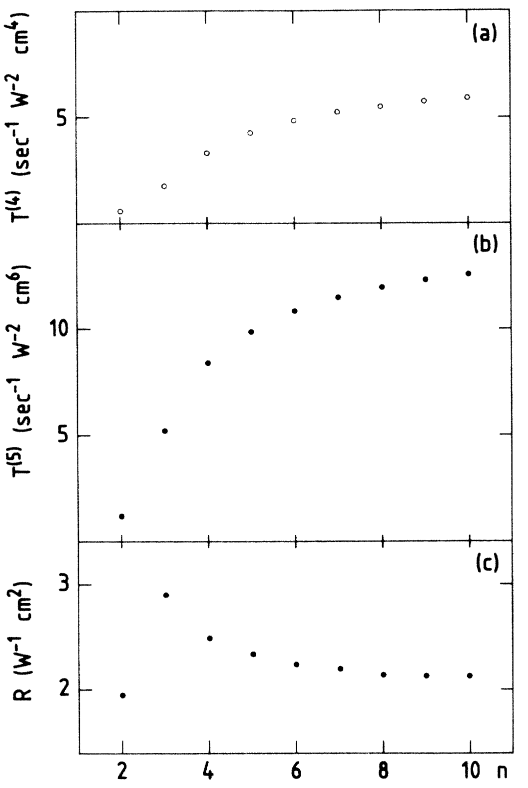

FIG. 6. (a) Transition rates $T=10^{31}W^{(4)}/I^2$ (in units of $\sec^{-1}\,\mathrm{W}^{-2}\,\mathrm{cm}^4$) of four-photon ionization (shown with open circles) for different resonant states. Principal quantum number n of the resonant np state is taken from $n=2$ to 10. (b) Closed circles are transition rates $T=(W^{(5)}\times 10^{46})/I^3$ (in units of $\sec^{-1}\,\mathrm{W}^{-3}\,\mathrm{cm}^6$) of the five-photon ionization, with one photon being entirely absorbed in the continuum. (c) Branching ratios $R=10^{15}W^{(5)}/W^{(4)}I$ (in units of $\mathrm{W}^{-1}\,\mathrm{cm}^2$) between the four- and five-photon ionization processes.

multiphoton ionization processes have been called above-threshold ionization (ATI).[17] In one practical case, the relevant process being REMPI, we may call it resonantly enhanced above-threshold ionization (REATI). At least one such experiment has been performed, as we shall see later.[13]

As long as the process occurs with relatively moderate laser intensity, the transition in the continuum can be described adequately by the perturbation theory, and the extension of the theory for REMPI to treat such processes is rather simple. One essentially needs to replace, in Eq. (8), the γ_j in the numerator by $\gamma_j^{(2)}$ [defined in Eq. (11b)], while the γ_j in the denominator has to be replaced by $\gamma_j^{(1)}$ [Eq. (10b)]. The obviousness of all this requires little explanation. One notes that the frequency dependence of REATI can then only be that of REMPI. The intensity dependence is also very simple. We have therefore decided to study REATI (at zero detuning) for its dependence on the principal quantum number n of the resonant state. The probability per unit time is given by

$$W^{(5)}=4\,|R_{ij}|^2\gamma_j^{(2)}/(\gamma_j^{(1)})^2\ , \tag{11a}$$

where

$$\gamma_j^{(2)}=2\pi(I/I_0)^2(\,|\langle E,p\,|D^-G_0D^-|\,np\rangle|^2 + |\langle E,f\,|D^-G_0D^-|\,np\rangle|^2)\ . \tag{11b}$$

We have made calculations for these processes for various values of n (up to $n=10$) for the same frequency as the one utilized for the calculations of four-photon ionization. The results are shown in Table I and Figs. 6(a) and 6(b). While the results are self-explanatory, we note that the increase of the probabilities with n is much faster than those calculated for the four-photon process. This leads to the nature of the branching ratio of these two processes (which is essentially the ratio $R=\gamma_j^{(2)}/(\gamma_j^{(1)}I)$ in units of cm^2/W. This is depicted in Fig. 6(c), which is a nonmonotonic function of n. It shows a rapid rise and then a falloff which becomes rather slow, essentially becoming a constant. Notice that for $n=3$, the branching ratio deviates by about 8% from its measured value reported in Ref. 13.

Summarizing the results presented in this section, a fairly clear qualitative picture of two fundamental processes for the hydrogen atom as a function of the principal quantum number of the resonant state has emerged from these calculations. It is possible to deduce from them the extrapolated values for very large n.

IV. COHERENCE AND PULSE-SHAPE EFFECTS

One aspect of calculations for multiphoton processes is that it is improbable that a theoretical estimate of the number of ions or total number of electrons, such as the ones reported in Secs. II and III, can be directly compared to measurements. The reason lies in the spatiotemporal structure of the laser pulses which have to be taken into account. These do modify the shapes of some of the curves shown above. Therefore, there is the need to examine carefully the modifications brought in by the realistic simulation of laboratory conditions. A second point that also merits some consideration is the changes in the probability due to the transition from a single-mode to a multimode laser.

We first investigate the effects of a general pulse shape[18] of the following kind:

$$I(R,Z,t)=I_M\frac{\exp[-R^2/(1+Z^2)]}{(1+Z^2)}[\cosh(2.63t/\tau)]^{-1}\ , \tag{12}$$

where I_M is the maximum intensity at the focus, $R=0.053r$ μm, and $Z=3.6z$ mm for a focus diameter of 53 μm. R and Z are the usual dimensionless cylindrical coordinates and τ represents the pulse width at half maximum. The reason for choosing this particular form is that this is an excellent prototype for pulse shapes of many experiments done currently in this area. Therefore calculations of the ionization probability $P_v(t,I_M,R,Z)$ with such spatio-temporal laser profiles serve as realistic illustrations of effects of the laser-pulse structure. The total ion number collected during a 9-nsec interaction time is shown in Fig. 7 (solid and dashed lines without open circles), and can then also be compared to the experimental data. The resonance profiles have been computed for three different intensities ($I_M = 1 \times 10^{10}$, 2×10^{10}, 3×10^{10} W/cm^2). Comparing Fig. 3 with Fig. 7, one immediately notes how the profiles are modified. The general effect of the pulse shape is to red shift the maxima and to change the shape of the curves to a slightly asymmetric one. It is not too difficult to understand these modifications. Since the intensity that the atom "perceives" is always less than I_M, all the "local" probabilities that go on to contribute to the "global" probabilities are seen to be red shifted, causing the asymmetry as well.

Finally, we go on to consider the case of the probabilities for a four-photon resonant-ionization process due to thermal (chaotic) light. Owing to the results of Ref. 19, we know that the dispersion curves corresponding to chaotic fields are blue shifted. Thus spatio-temporal effects contradict those resulting from light statistics. The aim of the last part of this paper is to evaluate the effects of these two conflicting shift mechanisms. Utilizing the well-known representation of coherent states, the probability $P_v(t,I_M,R,Z)$ can be expressed in the n-photon representation in the form $P_v(t,n,R,Z)$. The ionization probability computed with thermal light then reads

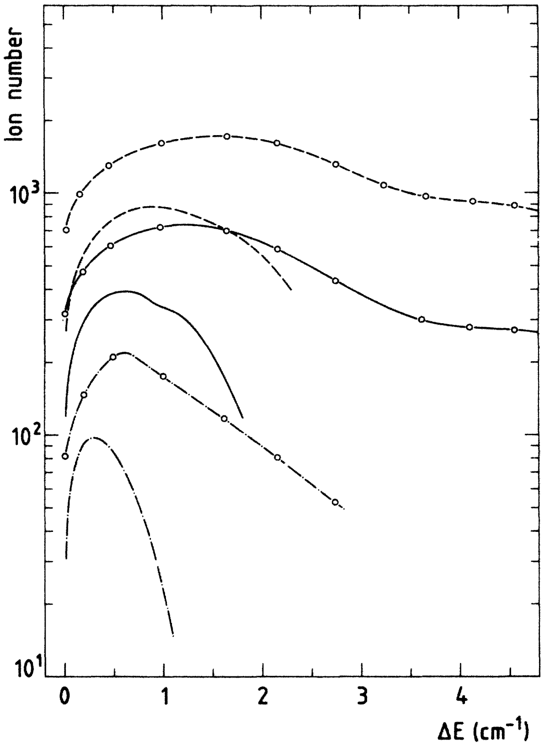

FIG. 7. Number of electrons produced for four-photon ionization of H with the effect of the spatio-temporal pulse shape of a laser taken into account at three different maximum intensities: (a) $I_M = 10^{10}$ W/cm^2 (—·—·—·), (b) $I_M = 2\times 10^{10}$ W/cm^2 (———), and (c) $I_M = 3\times 10^{10}$ W/cm^2 (— — —). The additional effect of chaotic light is also shown in this figure for the three mean intensities: (a) $\bar{I} = 10^{10}$ W/cm^2 (—○·—), (b) $\bar{I} = 2\times 10^{10}$ W/cm^2 (—○———○—), and (c) $\bar{I} = 3\times 10^{10}$ W/cm^2 (—○—○—). The interaction time is 9 nsec.

$$P_{\mathrm{th}}(t,\bar{n}) = \sum_{n=0}^{\infty} \frac{\bar{n}^n}{(1+\bar{n})^{n+1}} P_v(t,n) \ . \qquad (13)$$

The numerical problem in such summations is well known and has been solved as usual. The results are also shown in Fig. 7 at the same three intensities as before (lines with open circles). The tendency towards larger asymmetries is general in all the curves. A laser with 20 or more modes is sufficient to approximate the effects shown here. It might be of some interest also to study the gradual transition from a single mode to the chaotic-light limit, but we have not pursued that question.

It is of interest to compare some of our results with the existing experimental data. From the curves in Fig. 7, the width and the shift of the resonance profiles can be measured for thermal light. It can be easily seen that they are in excellent agreement with the results reported in Ref. 12. In addition, an analogous curve to those in Fig. 7 has been computed at $\bar{I} = 2.3\times 10^{10}$ W/cm^2 (7.1 mJ). After we normalized our results, we made the comparison between theory and experiment. The agreement is strikingly good and impossible to demonstrate graphically, since the two curves overlap one another. We conclude from this that the spatio-temporal structure of the laser pulse along with the assumption of thermal light explain the data very well.

V. CONCLUSION

We have considered the problem of resonant multiphoton ionization of atomic hydrogen with the intent of obtaining a certain number of significant new results as well as filling some lacunae in the literature. The calculations reported in this paper have been done for a pulse duration of 9 nsec. In this case, the ionization probability has a linear time dependence which can be seen in Fig. 2. From the relevant expression of the probability [Eq. (8)], we may clearly expect to have a resonant enhancement of the ionization profile. As has been shown in a previous paper,[20] this could not be the case for smaller interaction times in a region where the probability varies as the cube of time. It is not necessary to summarize all the results reported in this paper. We have investigated, in addition to the four-photon ionization via the $2p$ resonant state, the four- and five-photon ionization of H when three photons are in exact resonance with the np states ($n = 1,10$). In doing this, we have observed that the relevant probabilities are more and more slowly increasing functions of n. Then we have seen that, for weak values of the order of nonlinearity, the shift, the broadening, and the ionization probabilities can vary significantly in the interaction volume. This produces a red shift, a moderate broadening, and an asymmetry of the resonance profile which have been experimentally observed.[13] In contrast, the REMPI that is induced by a square and Gaussian laser pulse gives rise to a blue shift and a very large broadening of the resonance peak. These two effects combine to give results that are in excellent agreement with experiment. It is clear to us that the hydrogen atom, in combination with strong electromagnetic fields, reserves for us many interesting observables that have been only partly explored. A very recent experiment,[21] regarding the measurement of the angular distribution of the electrons produced in the above-threshold ionization and its corresponding calculation,[22] serve as one example of such.

ACKNOWLEDGMENT

The authors wish to thank Dr. C. Manus for constant encouragement during the course of this work.

---

[1] While it is impossible to give an exhaustive reference in this area, recent progress may be gauged by consulting the following: *Multiphoton Ionization of Atoms,* edited by S. L. Chin and P. Lambropoulos (Academic, New York, 1984); *Photons and Continuum States of Atoms and Molecules,* edited by N. K. Rahman, C. Guidotti, and M. Allegrini (Springer-Verlag, Berlin, 1986); Multielectron Excitations of Atoms, J. Opt. Soc. Am. B **4**, 5 (1987); Book of Abstracts of Proceedings of the International Conference on Multiphoton Ionization, Joint Institute for Laboratory Astrophysics, Boulder, 1987 (unpublished).

[2] B. L. Beers and L. Armstrong, Jr., Phys. Rev. **12**, 2447 (1975); L. Armstrong, Jr. and S. V. O'Neil, J. Phys. B **13**, 1125 (1980).

[3] A. E. Kazakov, V. P. Makarov, and M. V. Federov, Zh. Eksp. Teor. Fiz. **70**, 38 (1976) [Sov. Phys.—JETP **43**, 20 (1976)].

[4] M. V. Fedorov, J. Phys. B **10**, 2573 (1977).

[5] P. Lambropoulos, Phys. Rev. A **9**, 1992 (1974); S. N. Dixit and P. Lambropoulos, *ibid.* **19**, 1576 (1979).

[6] Shih-J. Chu and W. P. Reinhart, Phys. Rev. Lett. **39**, 1195 (1977).

[7] M. Crance, J. Phys. B **11**, 1931 (1978).

[8] J. L. F. de Meijere and J. H. Eberly, Phys. Rev. A **17**, 1416 (1978).

[9] W. A. McClean and S. Swain, J. Phys. B **11**, 1717 (1978).

[10] Y. Gontier and M. Trahin, Phys. Rev. A **19**, 2641 (1979).

[11] C. R. Holt, M. G. Raymer, and W. P. Reinhart, Phys. Rev. A **27**, 2971 (1983).

[12] D. K. Kelleher, M. Ligare, and L. R. Brewer, Phys. Rev. A **31**, 2747 (1985).

[13] M. J. Muller, H. B. van Linden van den Heuvell, and M. J. van der Wiel, Phys. Rev. A **34**, 236 (1986).

[14] Y. Gontier and M. Trahin, Phys. Rev. **172**, 83 (1968).

[15] A. Maquet, Phys. Rev. A **15**, 1088 (1977).

[16] N. K. Rahman, J. Phys. B **12**, 3229 (1979).

[17] Y. Gontier, M. Poirier, and M. Trahin, J. Phys. B **13**, 1381 (1980).

[18] A. L'Huillier, L. A. Lompré, G. Mainfray, and C. Manus, Phys. Rev. A **27**, 2503 (1983).

[19] Y. Gontier and M. Trahin, J. Phys. B **12**, 2123 (1979).

[20] Y. Gontier and M. Trahin, J. Phys. B **13**, 259 (1980).

[21] D. Feldmann, B. Wolff, M. Wenhöner, and K. H. Welge, Z. Phys. D **6**, 293 (1987).

[22] Y. Gontier, N. K. Rahman, and M. Trahin, Europhys. Lett. **5**, 595 (1988).